

Transition-State Charge Transfer Reveals Electrophilic, Ambiphilic, and Nucleophilic Carbon–Hydrogen Bond Activation

Daniel H. Ess,^{*,†,‡} Robert J. Nielsen,[†] William A. Goddard III,^{*,†} and Roy A. Periana^{*,‡}

Materials and Process Simulation Center, Beckman Institute, Division of Chemistry and Chemical Engineering, California Institute of Technology, Pasadena, California 91125, and The Scripps Research Institute, Jupiter, Florida 33458

Received April 6, 2009; E-mail: daniel@scripps.edu; wag@wag.caltech.edu; rperiana@scripps.edu

To capture the powerful potential of metal-mediated carbon–hydrogen (C–H) bond activation, it is essential to develop compatible reactions that convert the resulting metal–alkyl (M–R) intermediates into useful functionalized products.¹ For alkane oxidation reactions, Pt, Pd, Hg, and Au metal catalysts have been exploited to break C–H bonds by electrophilic activation.^{2,3} Because of the highly electrophilic C–H activation reactions, the resulting M–R intermediates react with weak O-nucleophiles to generate oxygenated products.² It has also recently been demonstrated that M–R intermediates can be functionalized with O-electrophiles.⁴ This type of M–R functionalization would be most useful if coupled to a nucleophilic C–H activation reaction.

In order to understand and classify the types of C–H activation reactions, here we report transition-state (TS) interaction energy decomposition calculations that quantify the direction and magnitude of charge transfer (CT) bonding between metal/ligand complexes and alkane C–H bonds. Analysis of complexes that are known to activate C–H bonds, encompassing Pt, Au, Ir, Ru, W, Sc, and Re metal centers, reveals that beyond the classic electrophilic (E) activation paradigm,^{2,3} there is a continuum that includes ambiphilic (A) as well as nucleophilic (N) activation (Figure 1). In using E, N, or A descriptors to classify the C–H activation TS, we are designating whether the metal/ligand fragment acts as an electrophile, nucleophile, or neither toward the C–H bond. In conjunction with the general phenomenological insertion (I) or substitution (S) descriptions of transition-state bonding,⁵ a straightforward perspective and classification scheme for C–H activation chemistry emerges.

All of the B3LYP geometries were optimized using Jaguar 7.5.^{6a} The Head-Gordon absolutely localized molecular orbital energy decomposition analysis (ALMO-EDA)^{6b} as implemented in a modified version of Q-Chem 3.1^{6c} was used to partition the interaction energies between the metal/ligand and CH₄ fragments in the TS geometries. This variational method utilizes block-localization of fragment MO coefficients and a perturbative single Roothaan step to obtain directional CT contributions (E_{CT}) as differences between localized and delocalized energies. The frozen-density energy (E_{FRZ}), a combination of Coulombic and exchange-correlation energies, and the fragment (intramolecular) polarization energy (E_{POL}) are also dissected in this analysis.

Figure 2 shows the diverse range of insertion and substitution C–H activation TSs that were analyzed, including oxidative addition, σ -bond metathesis, oxidative hydrogen migration or σ -CAM, and 1,2-substitution.^{1,7} Among these TSs, the total interaction energy E (the sum of all repulsions and stabilizations) and the total CT stabilization energy ($E_{CT1} + E_{CT2}$) between the

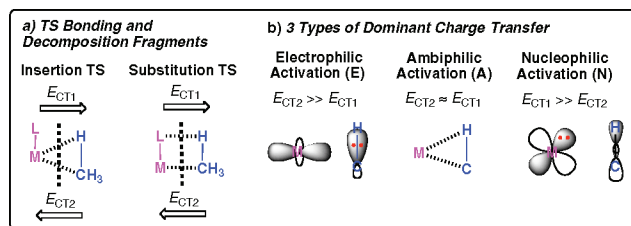


Figure 1. (a) Generalized insertion and substitution TS bonding and fragments used for decomposition analysis. (b) Generalized CT continuum of C–H bond activation for insertion.

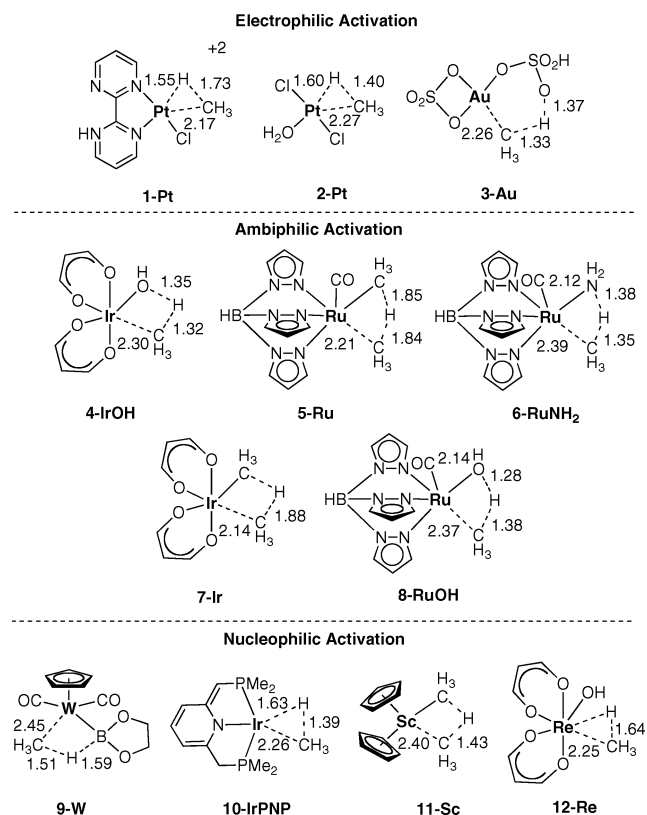


Figure 2. B3LYP/LACVP** TSs studied using ALMO-EDA. See the SI for an explanation of truncated ligands.

TS metal/ligand and CH₄ fragments (Table 1) are functions of reaction coordinate position, and both are correlated with the breaking C–H bond distance ($R^2 > 0.8$; Figure 3). These correlations enable the dominant TS CT interaction to be evaluated by the relative amounts of stabilization between the metal/ligand complex and methane ($\Delta E_{CT2-CT1}$), where E_{CT1} is the stabilization from metal/ligand to methane donation and E_{CT2} is the stabilization from

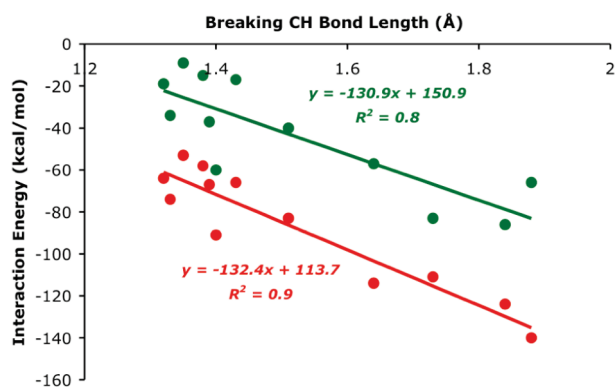
[†] California Institute of Technology.

[‡] The Scripps Research Institute.

Table 1. B3LYP/6-31G(d,p)[LANL2DZ] Transition State ALMO-EDA Results (kcal/mol)^{6d}

TS	E_{CT1}^a	E_{CT2}^b	E_{FRZ}	E_{POL}	E_{SE}^c	E_{HO}^d	E^e
1-Pt^f	-40 (-52)	-70 (-60)	53 (62)	-27 (-27)	3 (3)	-1 (-1)	-83 (-74)
2-Pt	-37	-55	50	-19	3	-3	-60
3-Au	-21	-52	73	-43	3	6	-34
4-IrOH	-25	-39	90	-46	2	-1	-19
5-Ru	-56	-68	84	-48	2	1	-86
6-RuNH₂	-28	-25	84	-41	3	-2	-9
7-Ir	-58	-54	68	-26	3	0	-66
8-RuOH	-32	-26	88	-47	4	-2	-15
9-W	-47	-35	66	-25	3	-1	-40
10-IrPNP	-40	-27	47	-18	2	-1	-37
11-Sc	-45	-21	80	-32	2	-1	-17
12-Re	-70	-44	79	-28	3	3	-57

^a Metal/ligand \rightarrow CH₄ CT stabilization energy. ^b CH₄ \rightarrow metal/ligand CT stabilization energy. ^c Basis set superposition energy. ^d Higher-order CT contribution that cannot be directionally separated. ^e Total TS interaction energy. ^f Values in parentheses are for the unprotonated **1-Pt** TS.

**Figure 3.** Linear correlations of transition state C–H bond length with total interaction energy (green) and total CT stabilization (red).

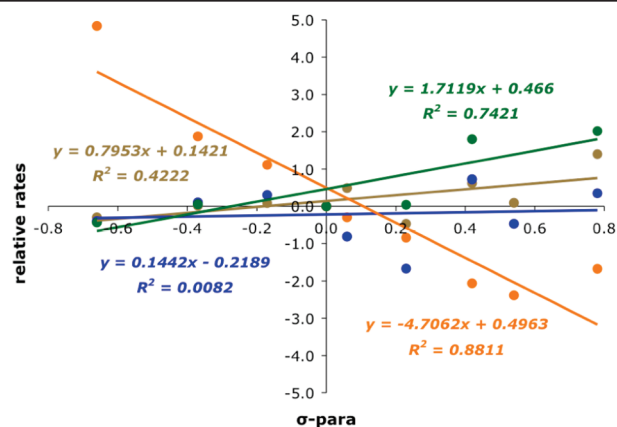
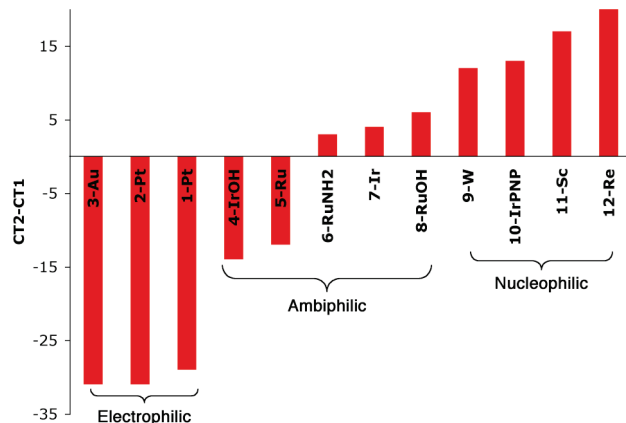
methane to metal/ligand donation (Figure 1). A negative $\Delta E_{CT2-CT1}$ value indicates an electrophilic mechanism, while a positive value indicates a nucleophilic mechanism. The repulsive E_{FRZ} terms depend on the exact transition structure and mitigate the CT and polarization stabilizations (E_{POL}).

The Catalytica [(H–bipyrimidine)Pt(II)Cl–CH₄]²⁺ transition state⁸ **1-Pt** (Figure 2), provides the archetypical example of C–H activation by electrophilic insertion (EI). The CH₄ \rightarrow (H–bipyrimidine)PtCl CT stabilization energy (E_{CT2}) is –70 kcal/mol, mainly as the result of the C–H σ -bond to empty d_{σ} orbital interaction. The stabilization energy for CT in the opposite direction (E_{CT1}) is –40 kcal/mol, resulting from donation into the C–H σ^* orbital. The difference in CT stabilization ($\Delta E_{CT2-CT1}$) is –30 kcal/mol, indicating electrophilic dominance.

Protonation of the distal bipyrimidine nitrogen in **1-Pt** enhances the electrophilic character of the (H–bipyrimidine)Pt(II)Cl TS fragment toward methane. In the unprotonated TS ((bipyrimidine)Pt(II)Cl–CH₄)⁺, $\Delta E_{CT2-CT1}$ decreases in magnitude to only –8 kcal/mol. The total CT stabilization in **1-Pt** and the unprotonated TS are approximately equal (see Table 1).

The (H₂O)Pt(II)Cl₂–CH₄ transition state **2-Pt**,⁹ typically described as arising from an oxidative addition mechanism, and the (HSO₄)(SO₄)Au(III)–CH₄ transition state **3-Au**² are both also highly electrophilic, with E_{CT1}/E_{CT2} ratios of \sim 1:2. **2-Pt** is another example of EI, while **3-Au** is an example of electrophilic substitution (ES).

The electrophilic nature of Au(III) substitution TSs was also confirmed with a computed theoretical Hammett plot for substitution

**Figure 4.** B3LYP gas-phase Hammett plots for benzylic C–H activation of substituted toluenes by (HSO₄)(SO₄)Au (orange), Tp(CO)RuNH₂ (blue), Tp(CO)RuOH (brown), and (PCP)Ir (green) complexes. Values of $\log(k_X/k_H)$ were plotted against the σ -para values for NO₂ (0.8), CF₃ (0.5), CHO (0.4), Cl (0.2), F (0.1), Me (–0.2), OH (–0.4), and NH₂ (–0.7). Free energies were computed as LACV3P**++ electronic energies using LACVP** geometries and free-energy corrections. A collision factor of 2.08×10^{10} and a gas constant (R) value of $1.984 \text{ cal K}^{-1} \text{ mol}^{-1}$ at 298 K were used.**Figure 5.** Plot of $\Delta E_{CT2-CT1}$, the difference between the forward and reverse CT stabilizations between the metal/ligand and methane fragments (kcal/mol), for the studied TSs.

into the benzylic C–H bond of para-substituted toluenes. The plot of $\log(k_X/k_H)$ against σ -para values gave a predicted ρ value of –4.7 (Figure 4) [see the Supporting Information (SI)].

Although Bergman's cationic [Cp*(L)IrMe]⁺ complexes are presumed to promote electrophilic C–H activation,¹⁰ analysis of the CH₄ insertion TS [Cp(PH₃)Ir(Me)–CH₄]⁺ (see the SI for structure and details) showed a $\Delta E_{CT2-CT1}$ value of only –12 kcal/mol. Compared with the Pt and Au systems, this system might better be described as breaking the C–H bond by an ambiphilic insertion (AI) TS (see below).

Analysis of several Ir and Ru complexes known to add to C–H bonds by so-called 1,2-substitution revealed a multitude of ambiphilic TSs. The TS energy decomposition results for (acac- κ O, κ O)₂–Ir–X [X = OH (**4-IrOH**), CH₃ (**7-Ir**)] and (CO)TpRu–X [X = CH₃ (**5-Ru**), NH₂ (**6-RuNH₂**), OH (**8-RuOH**)] complexes are given in Table 1.¹¹ Despite the differences in geometries and metal/ligand compositions among **4-IrOH**, **5-Ru**, **6-RuNH₂**, **7-Ir**, and **8-RuOH**, the differences between the forward and reverse CT in these TSs are much smaller than in the Pt and Au TSs, with $\Delta E_{CT2-CT1}$ values ranging from –14 to +6 kcal/mol. Figure 5 plots the $\Delta E_{CT2-CT1}$ values for all of the TSs shown in Figure 2 and clearly shows the change from electrophilic activation for Pt and Au complexes to a

region of ambiphilic activation for these Ir and Ru TSs. In **6-RuNH₂** and **7-Ir**, there is nearly equivalent CT between Tp(CO)Ru–NH₂ and (acac-κO,κO)₂Ir–CH₃, respectively, and CH₄, so these are examples of ambiphilic substitution (AS).

In this ambiphilic region of substitution TSs, better donor X groups do not necessarily lead to more favorable CT stabilization.¹² Comparison between the Ru–hydroxy and Ru–amido complexes (**8-RuOH** and **6-RuNH₂**, respectively) shows that for X = OH, $E_{CT1} = -32$ kcal/mol and $E_{CT2} = -26$ kcal/mol, while for X = NH₂, E_{CT1} and E_{CT2} decrease in magnitude to -28 and -25 kcal/mol, respectively. These results show that despite the classically predicted d_{π} – p_{π} repulsion model,¹³ better donor groups do not lead to greater CT stabilization in the TS. This is the case because a higher-energy occupied M–X π orbital may increase donation into the C–H σ^* orbital (potentially increasing E_{CT2}) but a simultaneous increase in X → M σ -bond donation decreases the electrophilicity of the metal (decreasing E_{CT1}). The opposite effect is also general: an increase in the metal center electrophilicity is mitigated by X → M σ -bond donation.^{12c}

The ambiphilic nature of these activation TSs is also manifested in the Hammett plots for Tp(CO)Ru–NH₂ and Tp(CO)Ru–OH with the benzylic C–H bond of substituted toluenes (Figure 4). In sharp contrast to the (HSO₄)(SO₄)Au complex, these plots exhibit ρ values of ~ 0 with essentially no R^2 correlation [see the SI for an (acac-κO,κO)₂Ir–OH Hammett plot].

The Cp(CO)₂W–B(O₂(CH₂)₂)–CH₄ transition state **9-W** begins a nucleophilic C–H activation regime where CT to methane dominates (Figure 5). The dearomatized (PNP)Ir(I)¹⁴ insertion transition state **10-IrPNP** and Cp₂ScMe alkyl metathesis¹⁵ transition state **11-Sc** show a more definitive crossover into nucleophilic C–H activation. E_{CT1} is now approximately twice as stabilizing as E_{CT2} because of low oxidation states and electropositive metals combined with more donating ligands. Although Cp₂Sc(III)Me is a d^0 system, the nucleophilic character of **11-Sc** reflects the dominating CT resulting from interaction of the Sc^{δ+}–Me^{δ-} polarized bond with the incoming methane. The reaction of (PNP*)Ir with methane can be described as a nucleophilic insertion (NI), while the W and Sc metathesis reactions are best described as nucleophilic substitutions (NS). Transition metals to the left of Ir and Ru on the periodic table are also likely to be involved in nucleophilic C–H activation. For example, an NI transition state is predicted for the (acac-κO,κO)₂-Re(III)–OH complex insertion into methane (**12-Re**), with a $\Delta E_{CT2-CT1}$ value of 26 kcal/mol.¹⁶ Although the alternative TS for this complex involving substitution across the Re–O bond is less energetically accessible,¹⁶ analysis of this TS actually shows a reversal of the electronic polarization, resulting in a TS with ES properties ($\Delta E_{CT2-CT1} = -16$ kcal/mol; see the SI). Analysis of the highly donating bis(hydrocarbyl)PCPIr(I) TS also shows a highly nucleophilic insertion TS ($\Delta E_{CT2-CT1} = -31$ kcal/mol; see the SI).¹⁷ The Hammett plot of (PCP)Ir with benzylic C–H bonds results in the expected positive ρ value of 1.7 (see Figure 4 and SI).

Analysis of [Pt(II)Cl₃–CH₄][–] and (HSO₄)Au(I)–CH₄ TSs also quantify how oxidation state and/or ligand exchange can alter the type of electronic activation. For example, the anionic Pt(II)Cl₃ complex, a potentially active species in the Shilov system at high chloride concentration,⁷ shows AI activation character with E_{CT1} and E_{CT2} values of -48 and -43 kcal/mol, respectively. Similarly, the change from Au(III) to Au(I) with a single bisulfate ligand also results in ambiphilic activation for the (HSO₄)Au(I)–CH₄ TS (see the SI).

Analysis of a diverse set of C–H activation transition states shows an electrophilic, ambiphilic, and nucleophilic CT continuum, which, importantly, influences the resulting M–R intermediate

polarization and choice of functionalization reaction. This analysis helps to classify the electronic characteristics of C–H activation systems and could impact the design of new C–H activation and compatible functionalization reactions.

Acknowledgment. Financial support was provided by Scripps Florida, Chevron, and DOE-EFRC.

Supporting Information Available: Complete ref 6c, ALMO-EDA results for TSs not shown in Figure 2, M06-DFT E_{CT} energies, explanation of model ligands, Cartesian coordinates, and absolute energies. This material is available free of charge via the Internet at <http://pubs.acs.org>.

References

- (1) (a) *Activation and Functionalization of C–H Bonds*; Goldberg, K. I., Goldman, A. S., Eds.; Oxford University Press: Washington, DC, 2004. (b) Bergman, R. G. *Nature* **2007**, *446*, 391, and references therein.
- (2) (a) Periana, R. A.; Taube, D. J.; Gamble, S.; Taube, H.; Satoh, T.; Fujii, H. *Science* **1998**, *280*, 560. (b) Periana, R. A.; Taube, D. J.; Evitt, E. R.; Loffler, D. G.; Wentreck, P. R.; Voss, G.; Masuda, T. *Science* **1993**, *259*, 340. (c) Periana, R. A.; Mironov, O.; Taube, D.; Bhalla, G.; Jones, C. J. *Science* **2003**, *301*, 814. (d) Jones, C. J.; Taube, D.; Ziatdinov, V. R.; Periana, R. A.; Nielsen, R. J.; Oxgaard, J.; Goddard, W. A., III. *Angew. Chem., Int. Ed.* **2004**, *43*, 4626.
- (3) (a) Gretz, E.; Oliver, T.; Sen, A. *J. Am. Chem. Soc.* **1987**, *109*, 8109. (b) Kao, L.-C.; Hutson, A. C.; Sen, A. *J. Am. Chem. Soc.* **1991**, *113*, 700. (c) Labinger, J. A.; Herring, A. M.; Bercaw, J. E. *J. Am. Chem. Soc.* **1990**, *112*, 5628. (d) Stahl, S. S.; Labinger, J. A.; Bercaw, J. E. *J. Am. Chem. Soc.* **1996**, *118*, 5961.
- (4) (a) Tenn, W. J., III; Conley, B. L.; Hövelmann, C. H.; Ahlquist, M.; Nielsen, R. J.; Ess, D. H.; Oxgaard, J.; Bischof, S. M.; Goddard, W. A., III; Periana, R. A. *J. Am. Chem. Soc.* **2009**, *131*, 2466. (b) Conley, B. L.; Ganesh, S. K.; Gonzales, J. M.; Ess, D. H.; Nielsen, R. J.; Ziatdinov, V. R.; Oxgaard, J.; Goddard, W. A., III; Periana, R. A. *Angew. Chem., Int. Ed.* **2008**, *47*, 7849.
- (5) (a) The term “substitution” is used here as a broad and accurate description of bonding involving the metal and ligand with the C–H bond. This term encompasses so-called “metathesis”. (b) Vastine, B. A.; Hall, M. B. *J. Am. Chem. Soc.* **2007**, *129*, 12068.
- (6) (a) *Jaguar*, version 7.0; Schrodinger, LLC: New York, 2007. (b) Khaliullin, R. Z.; Cobar, E. A.; Lochan, R. C.; Bell, A. T.; Head-Gordon, M. *J. Phys. Chem. A* **2007**, *111*, 10992. (c) Shao, Y.; et al. *Q-Chem*, version 3.1; Q-Chem, Inc.: Pittsburgh, PA, 2007. (d) The ALMO-EDA values in Table 1 have minimal basis-set and functional dependence. See Tables S1 and S3 in the SI for B3LYP/6-311++G(d,p) and M06/6-31G(d,p) comparisons.
- (7) For a recent review, see: Perutz, R. N.; Sabo-Etienne, S. *Angew. Chem., Int. Ed.* **2007**, *46*, 2578.
- (8) (a) Kua, J.; Xu, X.; Periana, R. A.; Goddard, W. A., III. *Organometallics* **2002**, *21*, 511. (b) Xu, X.; Kua, J.; Periana, R. A.; Goddard, W. A., III. *Organometallics* **2003**, *22*, 2057.
- (9) (a) Shilov, A. E.; Shul’pin, G. B. *Chem. Rev.* **1997**, *97*, 2879. (b) Zhu, H.; Ziegler, T. *J. Organomet. Chem.* **2006**, *691*, 4486.
- (10) (a) Tellers, D. M.; Yung, C. M.; Arndtsen, B. A.; Adamson, D. R.; Bergman, R. G. *J. Am. Chem. Soc.* **2002**, *124*, 1400. (b) Tellers, D. M.; Bergman, R. G. *Organometallics* **2001**, *20*, 4819.
- (11) For Ir–X substitution TSs, see: (a) Tenn, W. J., III; Young, K. J. H.; Oxgaard, J.; Nielsen, R. J.; Goddard, W. A., III; Periana, R. A. *Organometallics* **2006**, *25*, 5173. For Ru–X substitution TSs, see: (b) Cundari, T. R.; Grimes, T. V.; Gunnoe, T. B. *J. Am. Chem. Soc.* **2007**, *129*, 13172. (c) DeYonker, N. J.; Foley, N. A.; Cundari, T. R.; Gunnoe, T. B.; Petersen, J. L. *Organometallics* **2007**, *26*, 6604. Here, ρ values of ~ 2 were computed for benzene C–H activation by TpRu(L)(η^2 -C₆H₅X)Me complexes. (d) Conner, D.; Jayaprakash, K. N.; Wells, M. B.; Manzer, S.; Gunnoe, T. B.; Boyle, P. D. *Inorg. Chem.* **2003**, *42*, 4759. (e) Jayaprakash, K. N.; Conner, D.; Gunnoe, T. B. *Organometallics* **2001**, *20*, 5254. For W–X substitution TSs, see: (f) Webster, C. E.; Fan, Y.; Hall, M. B.; Kunz, D.; Hartwig, J. F. *J. Am. Chem. Soc.* **2003**, *125*, 858.
- (12) (a) Ryabov, A. D. *Chem. Rev.* **1990**, *90*, 403. (b) Canty, A. J.; van Koten, G. *Acc. Chem. Res.* **1995**, *28*, 406. (c) Ess, D. H.; Bischof, S. M.; Oxgaard, J.; Periana, R. P.; Goddard, W. A., III. *Organometallics* **2008**, *27*, 6440.
- (13) (a) Jayaprakash, K. N.; Gunnoe, T. B.; Boyle, P. D. *Inorg. Chem.* **2001**, *40*, 6481. (b) Mayer, J. M. *Comments Inorg. Chem.* **1988**, *8*, 125. (c) Holland, P. L.; Andersen, R. A.; Bergman, R. G. *Comments Inorg. Chem.* **1999**, *21*, 115.
- (14) (a) Ben-Ari, E.; Leitus, G.; Shimon, L. J. W.; Milstein, D. *J. Am. Chem. Soc.* **2006**, *128*, 15390.
- (15) (a) Sadow, A. D.; Tilley, T. D. *J. Am. Chem. Soc.* **2003**, *125*, 7971. (b) Sherer, E. C.; Cramer, C. J. *Organometallics* **2003**, *22*, 1682.
- (16) Gonzales, J. M.; Oxgaard, J.; Periana, R. A.; Goddard, W. A., III. *Organometallics* **2007**, *26*, 1505.
- (17) (a) Ghosh, R.; Emge, T. J.; Krogh-Jespersen, K.; Goldman, A. S. *J. Am. Chem. Soc.* **2008**, *130*, 11317. (b) Krogh-Jespersen, K.; Czerw, M.; Summa, N.; Renkema, K. B.; Achord, P. D.; Goldman, A. S. *J. Am. Chem. Soc.* **2002**, *124*, 11404.

JA902748C